Journal of Visualized Experiments

Perturbing Endothelial Biomechanics via Connexin 43 Structural Disruption
--Manuscript Draft--

Robert Steward Jr.
University of Central Florida
12760 Pegasus Drive
Bldg. 40, Room 245
Orlando, FL 32816-2450

June 27, 19

Phillip Steindel
Review Editor, Jove
1 Alewife Center, Suite 200
Cambridge, MA 02140

Dear Mr. Steindel,

Thank you for your consideration of our manuscript entitled "Protocol for perturbing endothelial biomechanics by Connexin 43 structural disruption". The authors of this paper Md. Mydul Islam and Robert Steward, Jr. very much appreciate your prompt response and the reviewer's comments. We have addressed the editor's comments and reviewer's comments point by point and highlighted each change in the manuscript in green. In addition, for your convenience and the reviewer's convenience we have also attached a document explicitly listing every change made to the manuscript in response to the reviewer's comments

We once again thank you for your consideration of our manuscript and look forward to hearing from you.

Sincerely,

Robert Steward Jr., Ph.D.

1   **TITLE:**
2   **Perturbing Endothelial Biomechanics via Connexin 43 Structural Disruption**
3
4   **AUTHORS AND AFFILIATIONS:**
5   M. M. Islam[1], R. L. Steward Jr.[1,2]
6   [1]Department of Mechanical and Aerospace Engineering, University of Central Florida, Orlando,
7   USA
8   [2]Burnett School of Biomedical Sciences, College of Medicine, University of Central Florida,
9   Orlando, USA
10
11 **Corresponding Author:**
12 R. L. Steward Jr.   (rstewardjr@ucf.edu)
13
14 **Email Address of Co-Author:**
15 M. M. Islam   (miku@knights.ucf.edu)
16
17 **KEYWORDS:**
18 Traction force microscopy, monolayer stress microscopy, mechanobiology, gap junction, Cx43,
19 intercellular stress
20
21 **SUMMARY:**
22 Here, we present a mechanics-based protocol to disrupt the gap junction connexin 43 and
23 measure the subsequent impact this has on endothelial biomechanics via observation of tractions
24 and intercellular stresses.
25
26 **ABSTRACT:**
27 Endothelial cells have been established to generate intercellular stresses and tractions, but the
28 role gap junctions play in endothelial intercellular stress and traction generation is currently
29 unknown. Therefore, we present here a mechanics-based protocol to probe the influence of gap
30 junction connexin 43 (Cx43) has on endothelial biomechanics by exposing confluent endothelial
31 monolayers to a known Cx43 inhibitor 2,5-dihydroxychalcone (chalcone) and measuring the
32 impact this inhibitor has on tractions and intercellular stresses. We present representative
33 results, which show a decrease in both tractions and intercellular stresses under a high chalcone
34 dosage (2 μg/mL) when compared to control. This protocol can be applied to not just Cx43, but
35 also other gap junctions as well, assuming the appropriate inhibitor is used. We believe this
36 protocol will be useful in the fields of cardiovascular and mechanobiology research.
37
38 **INTRODUCTION:**
39 The field that refers to the study of the effects of physical forces and of mechanical properties on
40 cellular and tissue physiology and pathology is known as mechanobiology[1]. A few useful
41 techniques that have been utilized in mechanobiology are monolayer stress microscopy and
42 traction force microscopy. Traction force microscopy allows for the computation of tractions
43 generated at the cell-substrate interface, while monolayer stress microscopy allows for the
44 computation of intercellular stresses generated between adjacent cells within a monolayer[2-6].

45 Results yielded from previous methods have suggested that cell-derived mechanical stresses play
46 a crucial role in determining the fate of a host of cellular processes[3-5]. For example, upon
47 exposure to an external mechanical force, a group of cells migrating as a collective can alter their
48 morphology and polarize their shape to align and migrate along the direction of applied force by,
49 in part, generating tractions[7,8]. Tractions provide a metric that can be used to evaluate cell
50 contractility and are calculated using traction force microscopy (TFM). Traction force microscopy
51 (TFM) begins with the determination of cell-induced substrate deformations followed by the
52 calculation of the traction field using a mathematically rigorous, mechanics-based computational
53 approach. Since the ability to calculate tractions has been around for quite some time,
54 researchers have utilized TFM to reveal the impact tractions have on a host of processes,
55 including cancer[9], wound healing[10] and assessment of engineered cardiac tissue[11].
56
57 Implementation of TFM and MSM together can be divided into three essential steps that must
58 be executed in the following order: first, the hydrogel deformations produced by the cells are
59 determined; second, tractions are recovered from hydrogel deformations; and third, a finite
60 element approach is used to compute normal and shear intercellular stresses within the entire
61 monolayer. To compute gel displacements, fluorescence bead images with cells were compared
62 with the reference bead image (without cells) by using a custom-written particle image
63 velocimetry (PIV) routine. The cross-correlation window size and overlap for PIV analysis were
64 chosen to be 32 x 32 pixels and 0.5, respectively. At this time, pixel shifts were converted into
65 microns by multiplying with a pixel-to-micron conversion factor (for our microscope, this
66 conversion factor is 0.65) to obtain in-plane displacements. Errors associated with ignoring out-
67 of-plane displacements are negligible[12,13]. After computation of gel displacements, there are two
68 types of traction measurements that can be utilized, constrained tractions and unconstrained
69 tractions[8,14]. Unconstrained tractions provide the traction field for the entire field of view
70 (including regions with and without cells), while constrained tractions provide the traction field
71 only for regions that include cells[14]. Then, intercellular stresses are calculated using monolayer
72 stress microscopy (MSM), which is an extension of traction force microscopy. Implementation of
73 MSM is based off the assumption that local tractions exerted by a monolayer of cells at the cell-
74 substrate interface must be balanced by mechanical forces transmitted between cells at the cell-
75 cell interface as demanded by Newton's laws[7,12,13]. A key assumption here is that the cell
76 monolayer can be treated as a thin elastic sheet because the traction distribution in the
77 monolayer is known and the force balance does not depend on cell material properties. Another
78 key assumption is that the traction forces are balanced by local intercellular stresses within the
79 optical field of view (within the monolayer) and the influence of this force balance is minimal in
80 the distal region (outside of the monolayer)[13]. Therefore, the boundary conditions defined by
81 intercellular stresses, displacements, or a combination of both at the monolayer boundary are
82 crucial to perform MSM[13].Taking into account the above information, we utilize MSM to perform
83 a finite element analysis (FEM) to recover the maximum principal stress (σ_{max}) and minimum
84 principal stress (σ_{min}) by rotating the stress plane at every point within the monolayer. These

85 principal stresses are subsequently used to compute the 2D average normal intercellular stress [
86 $(\sigma_{max} + \sigma_{min})$ /2] and 2D maximum shear intercellular stress [$(\sigma_{max} - \sigma_{min})$ /2] within the entire
87 monolayer[12,13]. This procedure is described in more detail by Tambe et al.[12,13]

89 Monolayer stress microscopy (MSM) allows for the calculation of cell-cell intercellular stresses
90 generated within a monolayer[6-8,12,13]. These intercellular stresses have been suggested to be
91 important for tissue growth and repair, wound healing, and cancer metastasis[12,15-17]. In addition,
92 intercellular stresses have been suggested to also be important in endothelial cell migration and
93 endothelial barrier function[17,18]. While cell-cell junctions such as tight junctions and adherens
94 junctions have both been suggested to play a critical role in endothelial intercellular stress
95 generation and transmission, the role of gap junctions remains elusive. Gap junctions physically
96 connect adjacent cells and provide a pathway for electrical current and molecules (<1 KDa) to
97 pass between neighboring cells[19-21]. Although endothelial cells express Cx37, Cx40, and Cx43 gap
98 junctions[19,22], Cx43 is arguably the most important in terms of disease progression[23]. Evidence of
99 Cx43's importance may be found in the fact that genetic deletion of Cx43 in mice results in
100 hypotension[24] and has adverse effects on angiogenesis[25]. In addition, Cx43 has been documented
101 to be important for cell migration and proliferation and in the progression of atherosclerosis[18,22-
102 25].

104 In this protocol, we used TFM and MSM to investigate whether traction and intercellular stress
105 generation within the confluent, endothelial monolayer would be impacted by the disruption of
106 the endothelial gap junction Cx43. We disrupted Cx43 with 2,5-dihydroxychalcone (chalcone), a
107 molecule documented to inhibit Cx43 expression[26]. Chalcone was used to disrupt Cx43 instead
108 of siRNA as chalcone has been reported previously by Lee et al. to disrupt Cx43 expression[26]. In
109 addition, we were particularly interested in chalcone's influence on the endothelium as it has
110 also been reported to be an anti-inflammatory and anti-platelet compound that can potentially
111 be used for the prevention and treatment of various vascular pathologies[26]. Chalcone treatments
112 were performed an hour after the experiment onset, chalcone-treated monolayers were imaged
113 for a total of six hours, and image processing was performed with a custom-written MATLAB code
114 to determine tractions and subsequently intercellular stresses. Our results showed an overall
115 decrease in tractions and intercellular stresses, suggesting Cx43 plays a key role in endothelial
116 biomechanics.

118 **PROTOCOL:**
119 **1. Making polyacrylamide (PA) gels**

121 **1.1. Preparation of Petri dish**
122

1.1.1. Prepare bind silane solution by mixing 200 mL ultrapure water with 80 µL acetic acid and 50 µL of 3-(trimethoxysilyl)propyl methacrylate. Bind silane is a solution used to functionalize the glass bottom Petri dish surface for hydrogel attachment.

1.1.2. Stir the bind silane solution on a stir plate for at least 1 h.

1.1.3. Treat the center well of the Petri dish with bind silane solution for 45 min.

1.1.4. Remove bind silane solution and rinse the Petri dish with ultra-pure water 2x–3x.

1.1.5. Dry the Petri dish surface and store at room temperature for future use.

1.2. Preparation of hydrogel solution

1.2.1. Mix ultra-pure water, 40% acrylamide, and 2% bis-acrylamide in a 15 mL centrifuge tube according to **Table 1**.

1.2.2. Add 80 µL of fluorescent beads to the hydrogel solution.

1.2.3. Gently shake the tube to mix beads with the gel solution.

1.2.4. Lightly tighten the tube cap on the centrifuge tube and place in a vacuum chamber.

1.2.5. Degas the gel solution for at least 45 min in vacuum chamber.

1.3. Hydrogel polymerization

1.3.1. First, add 75 µL of 10% ammonium persulfate (dissolved in ultra-pure water) and then add 8 µL of TEMED (N,N,N',N'-tetramethylethane-1,2-diamine) to the hydrogel solution.

1.3.2. Place 24 µL of hydrogel solution at the center of the Petri dish (see **Table 2**).

1.3.3. Use an 18 mm coverslip to flatten the hydrogel. This will give a height of ~100 µm.

1.3.4. Wait at least 30–40 min for gel polymerization.

1.3.5. Submerge the polymerized hydrogel in ultra-pure water to prevent gel dehydration.

1.3.6. Cover the Petri dish with aluminum foil to prevent photobleaching of fluorescent beads and store at 4 °C.

163

NOTE: Hydrogels can be stored a period of up to 3 months, but it is suggested that these gels be used no longer than 1 week after fabrication to obtain the best results.

2. Cell culture

2.1. Culture human umbilical vein endothelial cells (HUVECs) in cell culture medium 200 (see **Table of Materials**) supplemented with 1% penicillin-streptomycin on 0.1% gelatin-coated flasks at 37 °C and 5% CO_2.

3. Micropattern stencil preparation

3.1. Cure a thin layer of polydimethylsiloxane (PDMS) in a 100 mm Petri dish by mixing the silicone base with the silicone curing agent at a ratio of 20:1 (base: curing agent).

NOTE: It is possible to use other base to curing agent ratios (ex. 10:1 or 30:1). However, a lower base to curing agent ratio will yield a stiffer pattern, while a higher base to curing agent ratio will produce a softer pattern.

3.2. Prepare a 20:1 (base:curing agent) PDMS solution and mix carefully in a 50 mL centrifuge tube. Invert the tube upside down and shake vigorously multiple times to ensure proper mixing of the PDMS solution, as nonuniform mixing will result in incomplete polymerization.

3.3. Remove bubbles that have been introduced from the above step by centrifuging the PDMS solution for 1 min at 190 x *g*.

3.4. Pour 5–6 mL of PDMS solution in the center of a 100 mm Petri dish and agitate the dish until the PDMS solution covers the entire Petri dish surface.

3.5. Cure the PDMS solution overnight at 50–60 °C. PDMS can also be cured at room temperature.

3.6. Remove a circular, 16 mm diameter PDMS stencil with a hole puncher.

3.7. Use a biopsy punch to create small holes in the PDMS stencil. This protocol uses a 1.25 mm diameter biopsy punch.

3.8. Sterilize PDMS stencils by first submerging them in 70% ethanol for 2–3 min, aspirating off excess ethanol and then placing under a UV light for 5 min.

4. Collagen-I hydrogel coating

4.1. Remove the coverslip from the hydrogel and aspirate any excess liquid.

4.2. Place the PDMS stencil on the hydrogel surface.

NOTE: Tweezers can be used to apply light pressure to PDMS stencil to ensure a water-tight seal between the PDMS stencil and hydrogel surface. Our PDMS stencils are water-tight and thus prevent water access between the gel top surface and PDMS stencil bottom surface. Also, the hydrogel stiffness does not need to be adjusted with respect to the PDMS stiffness.

4.3. Cover the hydrogel surface with sulfosuccinimidyl-6-(4-azido-2-nitrophenylamino) hexanoate (sulfo-SANPAH) dissolved in a 0.1 M HEPES (4-(2-hydroxyethyl)-1-piperazineethanesulfonic acid) buffer solution at a concentration of 1 : 1000 and place under a UV lamp (power 36 W) for 8 min.

4.4. Aspirate the excess sulfo-SANPAH and HEPES solution and rinse the hydrogel twice with 0.1 M HEPES followed by an additional two rinses with ultra-pure water.

4.5. Aspirate excess ultra-pure water and coat hydrogels with 0.1 mg/mL collagen-I overnight at 4 °C.

4.6. Cover the dishes and protect fluorescent beads from photobleaching.

NOTE: PDMS stencils are used to create micropatterned monolayers. Micropatterned monolayers are utilized as they allow for multiple monolayers of the same geometry and dimensions to be observed simultaneously during each experiment. However, should micropatterns not be desired the above steps can be followed with the exception of step 4.2.

5. Creating HUVEC monolayers on hydrogels

5.1. Use 1x trypsin to detach cells from tissue culture flasks for 3–5 min in the incubator.

5.2. After trypsinization, add cell culture media to the trypsin solution and add to the 15 mL centrifuge tube.

5.3. Centrifuge the cell solution for 3 min at 1710 x g. A small, white pellet of cells should be visible at the bottom of the centrifuge tube.

242 5.4. Aspirate the supernatant and resuspend cells in media to a concentration of 50×10^4 cells/
243 mL.

245 5.5. Remove collagen-I from the hydrogel and rinse 1x with PBS.

247 5.6. Add 75×10^3 cells to the top of the PDMS stencil and allow cells to attach to the hydrogel
248 surface for at least 1 h in the incubator at 37 °C and 5% CO_2.

250 5.7. Remove the PDMS stencil and add at least 2 mL of media to the Petri dish. Submerge the
251 PDMS stencil in 10x trypsin to remove any attached cells and sterilize by spraying with 70%
252 ethanol and then placing under the UV light for 5 min.

254 5.8. Place the Petri dish in the incubator and wait at least 36 h or until a confluent monolayer is
255 observed.

257 **6. 2,5 dihydroxychalcone treatment for Cx43 disruption**

259 6.1. Dissolve 2,5 dihydroxychalcone (chalcone) in dimethylsulfoxide (DMSO) to make a 0.1875
260 mg/mL stock solution.

262 6.2. Dilute the stock solution with cell culture media to make a low chalcone concentration (0.2
263 µg/mL) aliquot and a high chalcone concentration (2 µg/mL) aliquot.

265 **7. Data acquisition**

267 7.1. Locate cell islands with a microscope.

269 7.2. Acquire phase contrast and bead images to image cell morphology and hydrogel
270 displacements, respectively.

272 NOTE: This protocol used a 10x objective for data acquisition.

274 7.3. At the end of the experiment, detach cells with 10x trypsin and acquire an image of the gel
275 surface without cells (reference image).

277 **8. Immunostaining**

279 8.1. Fix monolayers with 4% formaldehyde and incubate at 37 °C for 15 min.

281 8.2. Remove 4% formaldehyde and add 0.2% Triton X-100 for 5 min at 37 °C to permeabilize cells.

282
283 8.3. Remove 0.2% Triton X-100 and rinse monolayers with PBS 2x–3x.

284
285 8.4. Cover monolayer with 2% bovine serum albumin (BSA) solution for 45 min at 37 °C.

286
287 8.5. Remove the 2% BSA solution and rinse monolayers with PBS 2x–3x.

288
289 8.6. Add primary Cx43 antibody at a concentration of 1:400 to the sample and incubate overnight
290 at 4 °C.

291
292 8.7. Remove primary antibody and rinse sample with PBS 2x–3x.

293
294 8.8. Add secondary antibody at a concentration of 3:200 and incubate for 2 h at 37 °C.

295
296 NOTE: Samples should be covered to prevent photobleaching.

297
298 8.9. Remove secondary antibody and rinse with PBS 2x–3x.

299
300 8.10. Cover sample with mounting medium (Fluromount-G DAPI) and seal with an 18 mm cover
301 slip.

302
303 **9. Implementation of traction force microscopy (TFM) and monolayer stress microscopy (MSM)**

304
305 **9.1. Hydrogel deformation calculation**

306
307 NOTE: A step-by-step displacement calculation procedure using MATLAB is given below.

308
309 9.1.1. Open the main **traction.m** file in MATLAB (for all the MATLAB routines see Supplementary
310 Materials).

311
312 NOTE: Follow instructions provided in the code to set the MATLAB directory.

313
314 9.1.2. Define the following variables: image format, pixel-to-micron conversion, Young's
315 modulus, Poisson's ratio, and microscope objective.

316
317 9.1.3. Locate the bead, trypsin image, and phase image using the **OpenFiles** subroutine.

318
319 NOTE: For large data sets, it is best to name files in sequential order. For example,
320 files should be named "filename1.tif", "filename2.tif", etc.

321

322   9.1.4. Define a square ROI (region of interest) around the cell monolayer and execute the
323   **cell_cropper** subroutine to crop the original image.

324

325   9.1.5. Execute the **displacement_finder** subroutine to compute displacements.

326

327   9.1.6. Execute the **Dedrift** subroutine to remove any additional non-cellular displacements that
328   may be due to microscope stage drift.

329

330   **9.2. Computation of tractions**

331

332   NOTE: Here, unconstrained tractions are calculated using our custom-written MATLAB routine.
333   Step by step traction computation using the MATLAB routine previously mentioned is given
334   below.

335

336   9.2.1. Define the following variables within the **traction.m** routine: boundary condition, gel
337   thickness, gel height, and dedrift.

338

339   9.2.2. Execute the **traction_finder** subroutine to calculate tractions and execute the
340   **plot_traction** subroutine to plot tractions. All the tractions in x-direction (Tx) and y-direction (Ty)
341   along with their corresponding pixel locations can be found in a traction.dat file that will be
342   generated by the code.

343

344   **9.3. Computation of intercellular stresses**

345

346   NOTE: Step by step instructions for intercellular stress computation using the MATLAB routine
347   previously mentioned are given below.

348

349   9.3.1. Execute the **mark_circular_domain** subroutine to specify the monolayer boundary. This
350   routine will prompt all cropped phase images sequentially for the user to manually draw a
351   boundary around the monolayer. Keep a note of the nXPts generated in command window and
352   use them later as grid parameters in both X axis and Y axis for FEM analysis (see step 9.3.2).

353

354   9.3.2. Execute **Run_StressCode** to compute intercellular stresses. This subroutine directly reads
355   parameters from "model.in" file and executes "island.exe" to perform FEM analysis. Before
356   running this routine, make sure all parameters in the **model.in** file, i.e. grid parameters in X and
357   Y, pixel to micron conversion, Young's modulus of the gel, Poisson's ratio, monolayer height, and
358   monolayer pattern (strip or hole), are edited correctly.

359

360   9.3.3. Plot all the FEM results using the **plot_FEM_results** subroutine.

361

362   NOTE: All results generated will automatically be stored in the **Results** folder in the MATLAB
363   directory.

364

365   **REPRESENTATIVE RESULTS:**
366   Phase contrast images of control, 0.2 µg/mL, and 2 µg/mL chalcone treated monolayers were
367   taken 30 minutes before chalcone treatment (**Figure 1A–C**) and 2 hours after chalcone treatment
368   (**Figure 1D–F**). Cell-induced bead displacements (µm) were observed to decrease in both low
369   dose chalcone and high dose chalcone conditions (**Figure 2E,F**) when compared to control HUVEC
370   monolayers (**Figure 2D**). Prior to chalcone treatment, rms tractions were around 51 ± 8 Pa (**Figure
371   3A–C**) for all conditions. After chalcone treatment, there was a small increase in rms tractions to
372   59 ± 11 Pa in a low dose chalcone treated monolayers (**Figure 3E**) and an almost 2-fold decrease
373   in rms tractions to 18 ± 2 in high dose chalcone treated monolayers (**Figure 3F**) compared to the
374   control (**Figure 3D**). Prior to chalcone treatment, average normal intercellular stresses were
375   around 220 ± 66 Pa (**Figure 4A–C**). After chalcone treatment, there was an increase in average
376   normal intercellular stress magnitude to 285 ± 75 Pa with low dose chalcone treatment (**Figure
377   4E**) but a significant decrease in average normal intercellular stress magnitude to 106 ± 4 Pa with
378   high dose chalcone treatment (**Figure 4F**) when compared to control average normal intercellular
379   stresses (235 ± 18 Pa, **Figure 4D**). Maximum shear intercellular stresses were around 241 ± 30 Pa
380   (**Figure 5A–C**) before chalcone treatment, but after the chalcone treatment, there was a decrease
381   to 227 ± 20 Pa at low chalcone concentration (**Figure 5E**) and a further decrease in maximum
382   shear intercellular stress magnitude to 91 ± 6 Pa at high chalcone concentration treatment
383   (**Figure 5F**) when compared to control maximum shear intercellular stresses (270 ± 30 Pa, **Figure
384   5D**). The analysis of tractions and intercellular stresses are presented in **Figure 6A–C.** All plotted
385   results were tested for statistical significance (t-test and single factor ANOVA test), and in both
386   tests results were found to be statistically significant ($p < 0.05$) when independently comparing
387   0.2 µg/mL chalcone concentration and 2 µg/mL chalcone to control conditions (without
388   chalcone).

389

390   **FIGURE AND TABLE LEGENDS:**

391

392   **Figure 1: Representative phase contrast images of HUVEC monolayers.** Example phase contrast
393   images of control HUVECs at 30 min (**A**) and 2 h (**D**), phase contrast images of HUVECs treated
394   with 0.2 µg/mL chalcone at 30 min (**B**) and 2 h (**E**), and phase contrast images of HUVECs treated
395   with 2 µg/mL chalcone at 30 min (**C**) and 2 h (**F**) of experiment onset. Scale bar represents the
396   monolayer diameter of 1.25 mm.

397

398   **Figure 2: Illustration of displacement field produced by HUVEC monolayers.** Representative
399   displacements (µm) of control HUVECs at 30 min (**A**) and 2 h (**D**), HUVECs treated with 0.2µg/mL
400   chalcone at 30 min (**B**) and 2 h (**E**), and HUVECs treated with 2 µg/mL chalcone at 30 min (**C**) and

401 2 h (**F**) of experiment onset. Scale bar represents the monolayer diameter of 1.25 mm. Color bar
402 represents displacements in µm.

404 **Figure 3: RMS traction distribution in HUVEC monolayers.** Example of rms tractions (Pa) of
405 control, 0.2 µg/mL chalcone, and 2 µg/mL chalcone HUVECs before chalcone treatment (**A–C**)
406 and after an hour of chalcone treatment (**D–F**), respectively. Scale bar represents the monolayer
407 diameter of 1.25 mm. Color bar represents RMS tractions in Pa.

409 **Figure 4: Average Normal Intercellular Stress distribution in HUVEC monolayers.** Average
410 normal intercellular stress (Pa) distribution of control HUVECs at 30 min (**A**) and 2 h (**D**), HUVECs
411 treated with 0.2 µg/mL chalcone at 30 min (**B**) and 2 h (**E**), and HUVECs treated with 2 µg/mL
412 chalcone at 30 min (**C**) and 2 h (**F**). Scale bar represents the monolayer diameter of 1.25 mm.
413 Color bar represents stresses in Pa.

415 **Figure 5: Maximum Shear Intercellular Stress distribution in HUVEC monolayers.** Maximum
416 shear intercellular stress (Pa) distribution of control HUVECs at 30 min (**A**) and 2 h (**D**), HUVECs
417 treated with 0.2µg/mL chalcone at 30 min (**B**) and 2 h (**E**), and HUVECs treated with 2 µg/mL
418 chalcone at 30 min (**C**) and 2 h (**F**). Scale bar represents the monolayer diameter of 1.25 mm.
419 Color bar represents stresses in Pa.

421 **Figure 6: Comparison of RMS tractions and Intercellular Stresses in HUVEC monolayers and**
422 **impact of chalcone treatment on HUVEC gap junction Cx43 structures.** Plots of average normal
423 intercellular stress (**A**), maximum shear intercellular stress (**B**) and RMS tractions (**C**) show the
424 impact of chalcone doses (0.2 µg/mL and 2 µg/mL) on HUVEC monolayers compared to control.
425 Error bars show standard error. Results were found to be statistically significant (sample size = 6
426 islands, with a confidence level of 95%) using both t-tests compared to control ($p < 0.05$) and
427 single factor ANOVA ($p < 0.05$). In separate dishes, immunostaining was performed 5 h post-
428 addition of the drug for islands of cells residing on soft 1.2 kPa hydrogels. The green color
429 represents Cx43 and blue represents DAPI (nucleus). Panel **D** depicts the following: control (**E,H**),
430 0.2 µg/mL chalcone treated cells (**F,I**) and 2µg/mL chalcone treated cells (**G,J**). Scale bar = 200
431 µm, objective = 20x.

433 **Supplementary Figure 1: High resolution Cx43 staining in HUVEC monolayers.** Fixed HUVEC
434 monolayers were stained for Cx43 (green) and nucleus (DAPI, blue) to observe the dose-
435 dependent effect of chalcone. Higher magnification images (63x objective) reveal Cx43
436 localization mostly around the nucleus (evident from green fluorescence intensity). Shown are
437 control (**A–C**), 0.2 µg/mL chalcone treated cells (**D-F**) and 2 µg/mL chalcone treated cells (**G–I**).
438 Scale bar = 100 µm, objective = 63x oil immersion.

440 **Table 1: Polyacrylamide gel making formulations for different Young's moduli.**

441

Table 2: Gel volume and thickness.

442

443

444 **DISCUSSION:**

445 Our group, as well as others, has been successfully using TFM and MSM to probe the influence
446 of cell-cell junctions in various pathological and physiological cellular processes in vitro[7,15,18,27].
447 For example, Hardin et al. presented a very insightful study that suggests intercellular stress
448 transmission guides paracellular gap formation in endothelial cells[15]. While it possible to relate
449 the Cx43-related changes we report here to the changes reported by Hardin et al., we do not
450 specifically address paracellular gap formation in this protocol. Here, we presented a mechanics-
451 based protocol to specifically target the gap junction Cx43 and investigate its influence on
452 endothelial biomechanics.

453

454 To make this protocol successful, there were a few challenges that we had to overcome, some of
455 which could occur should other researchers decide to adopt our protocol for similar studies. A
456 major challenge was to find an optimum chalcone dose range where Cx43 expression could be
457 inhibited, while simultaneously keeping our endothelial monolayers intact. The IC50 of chalcone
458 for HUVECs has previously been reported to be 10.01 µg/mL[28]. However, when we exposed our
459 HUVEC monolayers to multiple chalcone concentrations ranging from 0.2 µg/mL to 20 µg/mL, we
460 found a chalcone concentration of 2 µg/mL to be the highest concentration our monolayers could
461 withstand while still remaining confluent. A confluent monolayer was essential for this protocol,
462 as a monolayer is required to measure intercellular stresses using MSM. Next, we performed an
463 immunofluorescence assay to determine if the selected doses of chalcone successfully disrupted
464 Cx43 structure or apparent expression. Our result revealed that while disruption of Cx43
465 structure with 0.2 µg/mL chalcone was visually difficult to distinguish from control, cells treated
466 with 2 µg/mL of chalcone appeared to show an apparent difference in Cx43 structure and
467 potentially expression (**Figure 6D** and **Supplementary Figure 1**). In addition, our results showed
468 that Cx43 disruption indeed influences endothelial biomechanics by reducing tractions and
469 intercellular stresses at its highest concentration. These findings are in agreement with
470 Bazellieres et al. who showed silencing of Cx43 with siRNA to also reduce tractions and
471 intercellular stresses, but in a sheet of epithelial cells[27]. Although our results are in agreement
472 with others it should be noted that the molecule we used to disrupt Cx43 expression, chalcone,
473 has also been suggested to influence activation of MAPK and NFkB in addition to Cx43
474 disruption[26]. Therefore, since we did not specifically look at the above-mentioned molecules or
475 their associated pathways, we cannot rule out the influence a potential MAPK and NFkB
476 perturbation can have on endothelial biomechanics as well.

477

478 Another key point worth mentioning is that the recovered tractions and intercellular stresses are
479 2D in nature and ignore out of plane (z-direction) tractions and intercellular stresses[12,13]. While
480 there is a small error associated with ignoring out-of-plane stresses, this error is negligible[13]. In

481 addition, the lateral dimension of the monolayer is sufficiently large (1.25 mm) relative to the
482 monolayer height (~ 5 μm) such that we would not expect significant displacements in the z-
483 direction. Furthermore, the MSM calculation offers error at the monolayer boundary[12,13].
484 However, Tambe et al. experimentally showed that errors are highest at the optical edges (i.e.,
485 the monolayer boundary) and decays quickly distal from boundary edges[13]. We perform
486 micropatterning and then calculate intercellular stresses of the entire monolayer to avoid
487 boundary errors that can occur during intercellular stress computation.
488
489 Monolayer stress microscopy is utilized in this protocol as the intercellular stress information
490 yielded from this method is essential in order to have a more complete understanding of the role
491 gap junction disruption has on endothelial biomechanics. In addition, intercellular stresses have
492 been suggested to be important in endothelial barrier function, as suggested by Hardin et al.[15]
493 and Krishnan et al.[17], for example. Furthermore, while intercellular stresses were correlated to
494 tractions in the representative data presented here, this is not always the case depending on the
495 stimulus. In the study of Steward et al., for example, endothelial intercellular stresses were
496 shown to decrease under fluid shear, while tractions remained relatively unchanged[7]. Also, the
497 protocol we present here does not allow for the simultaneous measurement of cell-derived
498 mechanical forces and staining of junctions and focal adhesions, but such an addition would be
499 complimentary to this protocol. In closing, the protocol we present here describes a mechanics-
500 based method to investigate the influence Cx43 has solely on endothelial biomechanics,
501 specifically endothelial cell-derived forces. We believe our mechanics-based protocol can be used
502 in conjunction with currently existing biological-based protocols to provide truly groundbreaking
503 work in the field.
504
505 **ACKNOWLEDGEMENTS:**
508
509 **DISCLOSURES:**
510 The authors have nothing to disclose.
511
512 **REFERENCES:**
513   1. Mammoto, T., Mammoto, A., Ingber, D. E. Mechanobiology and developmental control.
514   *Annual Review of Cell and Developmental Biology.* **29**, 27-61 (2013).
515   2. Schwarz, U. S., Soine, J. R. Traction force microscopy on soft elastic substrates: A guide to
516   recent computational advances. *Biochimica et Biophysica Acta.* **1853** (11 Pt B), 3095-3104
517   (2015).
518   3. Style, R. W. et al. Traction force microscopy in physics and biology. *Soft Matter.* **10** (23),
519   4047-4055 (2014).

4. Colin-York, H. et al. Super-Resolved Traction Force Microscopy (STFM). *Nano Letters.* **16** (4), 2633-2638 (2016).

5. Zimmermann, J. et al. Intercellular stress reconstitution from traction force data. *Biophysical Journal.* **107** (3), 548-554 (2014).

6. M.M. Islam. Recent Advances in Experimental Methods of Cellular Force Sensing. *Biomedical Journal of Science & Technical Research.* **17** (3), DOI: 10.26717/BJSTR.2019.17.002992 (2019).

7. Steward, R., Jr., Tambe, D., Hardin, C. C., Krishnan, R., Fredberg, J. J. Fluid shear, intercellular stress, and endothelial cell alignment. *American Journal of Physiology-Cell Physiology.* **308** (8), C657-664 (2015).

8. Trepat, X. et al. Physical forces during collective cell migration. *Nature Physics.* **5**, 426-430 (2009).

9. Li, Z. et al. Cellular traction forces: a useful parameter in cancer research. *Nanoscale.* **9** (48), 19039-19044 (2017).

10. Brugues, A. et al. Forces driving epithelial wound healing. *Nature Physics.* **10** (9), 683-690 (2014).

11. Pasqualini, F. S. et al. Traction force microscopy of engineered cardiac tissues. *PLoS One.* **13** (3), e0194706 (2018).

12. Tambe, D. T. et al. Collective cell guidance by cooperative intercellular forces. *Nature Materials.* **10** (6), 469-475 (2011).

13. Tambe, D. T. et al. Monolayer stress microscopy: limitations, artifacts, and accuracy of recovered intercellular stresses. *PLoS One.* **8** (2), e55172 (2013).

14. Butler, J. P., Tolic-Norrelykke, I. M., Fabry, B., Fredberg, J. J. Traction fields, moments, and strain energy that cells exert on their surroundings. *American Journal of Physiology-Cell Physiology.* **282** (3), C595-605 (2002).

15. Hardin, C. C. et al. Long-range stress transmission guides endothelial gap formation. *Biochemical and Biophysical Research Communications.* **495** (1), 749-754 (2018).

16. Cho, Y., Son, M., Jeong, H., Shin, J. H. Electric field-induced migration and intercellular stress alignment in a collective epithelial monolayer. *Molecular Biology of the Cell.* **29** (19), 2292-2302 (2018).

17. Krishnan, R. et al. Substrate stiffening promotes endothelial monolayer disruption through enhanced physical forces. *American Journal of Physiology-Cell Physiology.* **300** (1), C146-154 (2011).

18. Islam, M.M., Steward, R.L. Probing Endothelial Cell Mechanics through Connexin 43 Disruption. *Experimental Mechanics.* **59**, 327, https://doi.org/10.1007/s11340-018-00445-4 (2019)

19. Figueroa, X. F., Duling, B. R. Gap junctions in the control of vascular function. *Antioxidants & Redox Signaling.* **11** (2), 251-266 (2009).

20. Nielsen, M. S. et al. Gap junctions. *Comprehensive Physiology.* **2** (3), 1981-2035 (2012).

559 21. Sohl, G., Willecke, K. Gap junctions and the connexin protein family. *Cardiovascular*
560   *Research.* **62** (2), 228-232 (2004).
561 22. Haefliger, J. A., Nicod, P., Meda, P. Contribution of connexins to the function of the
562   vascular wall. *Cardiovascular Research.* **62** (2), 345-356 (2004).
563 23. Marquez-Rosado, L., Solan, J. L., Dunn, C. A., Norris, R. P., Lampe, P. D. Connexin43
564   phosphorylation in brain, cardiac, endothelial and epithelial tissues. *Biochimica et*
565   *Biophysica Acta.* **1818** (8), 1985-1992 (2012).
566 24. Liao, Y., Day, K. H., Damon, D. N., Duling, B. R. Endothelial cell-specific knockout of
567   connexin 43 causes hypotension and bradycardia in mice. *Proceeding of the National*
568   *Academy of Sciences of the United States of America.* **98** (17), 9989-9994 (2001).
569 25. Walker, D. L., Vacha, S. J., Kirby, M. L., Lo, C. W. Connexin43 deficiency causes
570   dysregulation of coronary vasculogenesis. *Developmental Biology.* **284** (2), 479-498
571   (2005).
572 26. Lee, Y. N. et al. 2',5'-Dihydroxychalcone down-regulates endothelial connexin43 gap
573   junctions and affects MAP kinase activation. *Toxicology.* **179** (1-2), 51-60 (2002).
574 27. Bazellieres, E. et al. Control of cell-cell forces and collective cell dynamics by the
575   intercellular adhesome. *Nature Cell Biology.* **17** (4), 409-420 (2015)
576 28. Nam, N. H. et al. Synthesis and cytotoxicity of 2,5-dihydroxychalcones and related
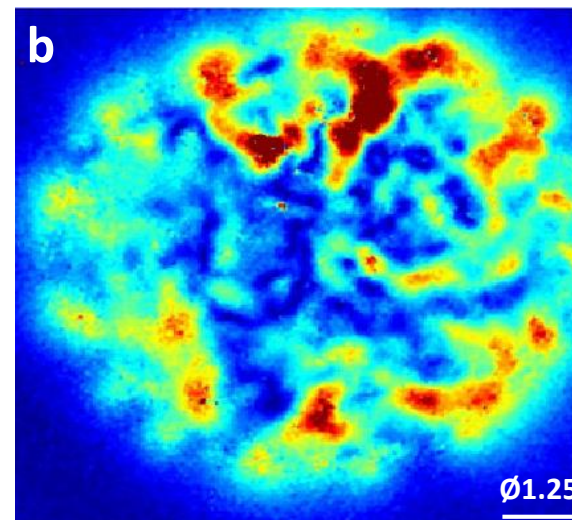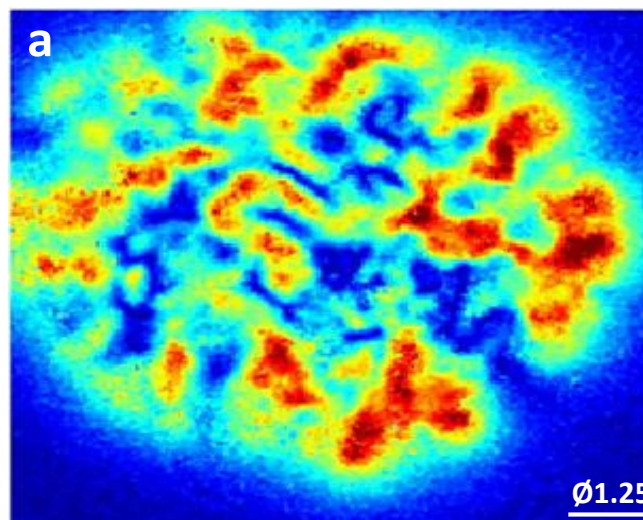577   compounds. *Archives of Pharmacal Research.* **27** (6), 581-588 (2004).
578
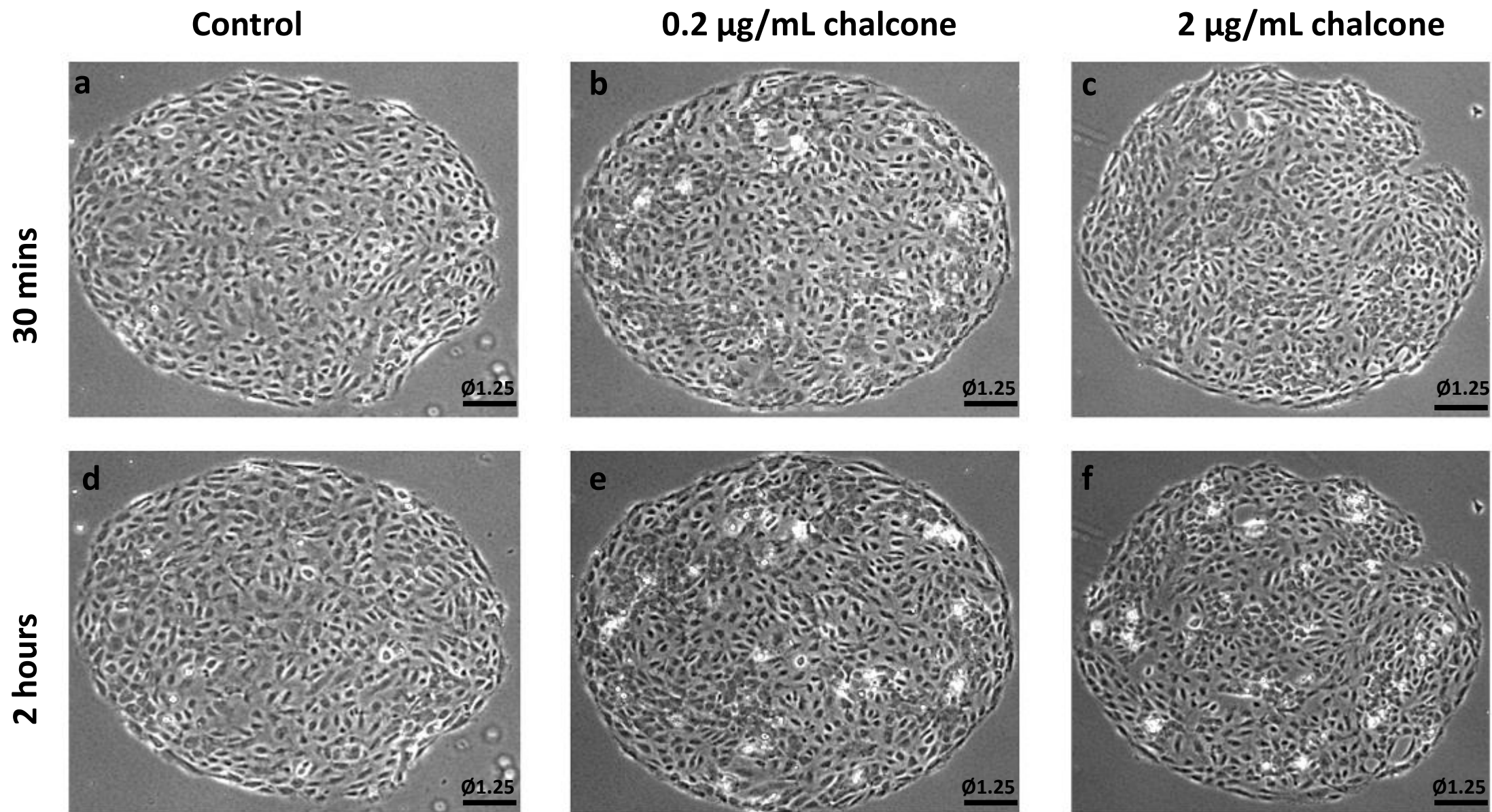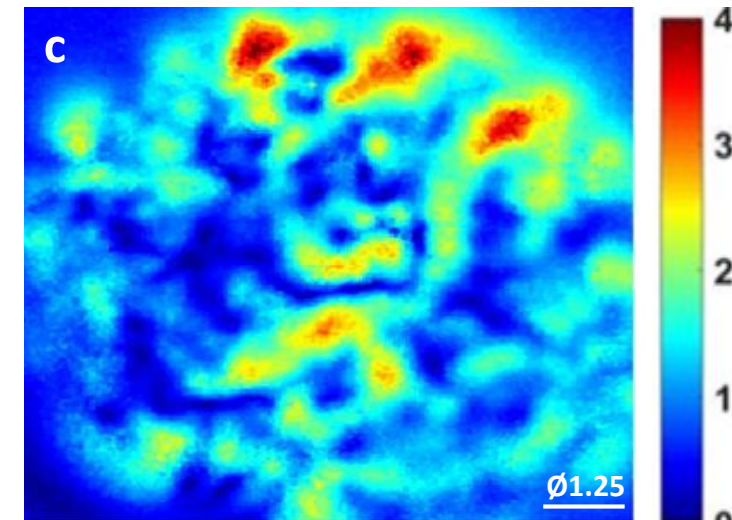
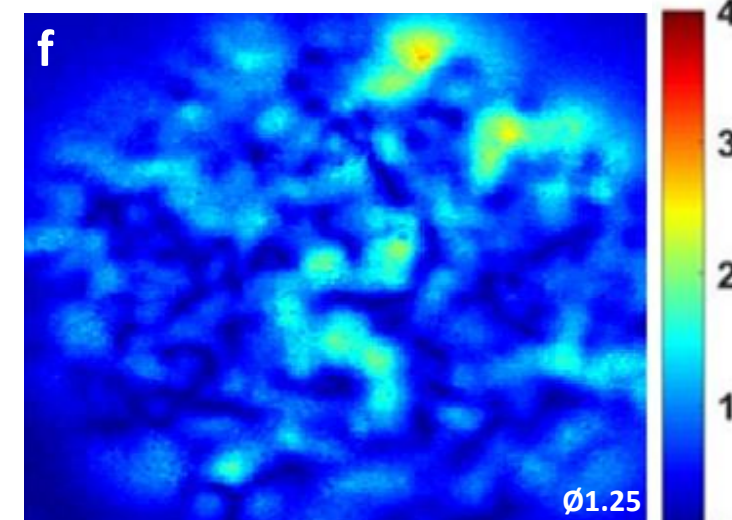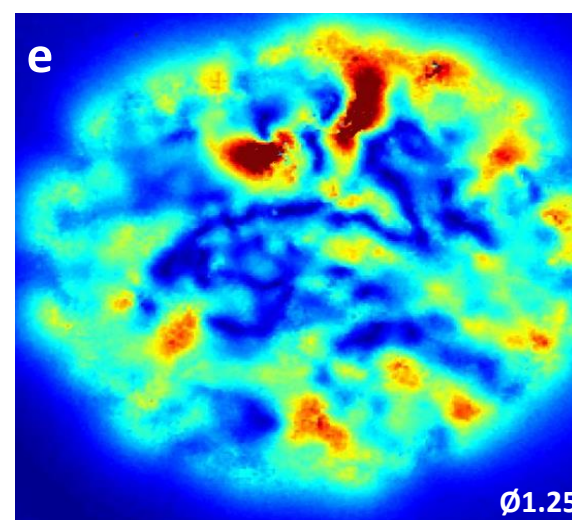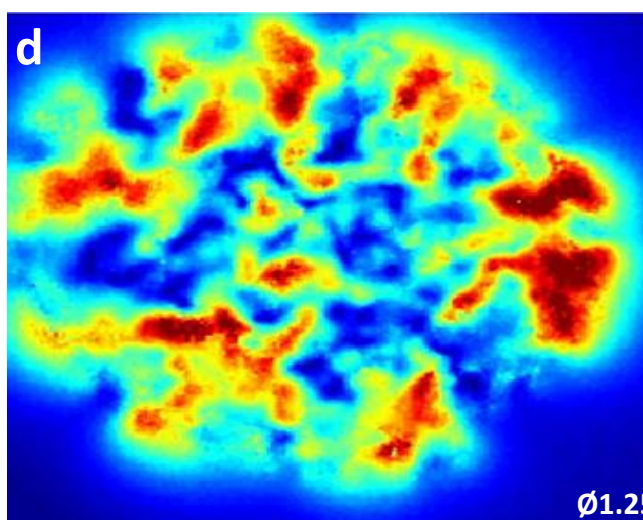| Control	0.2 µg/mL chalcone	2 µg/mL chalcone

Displacements (μm)
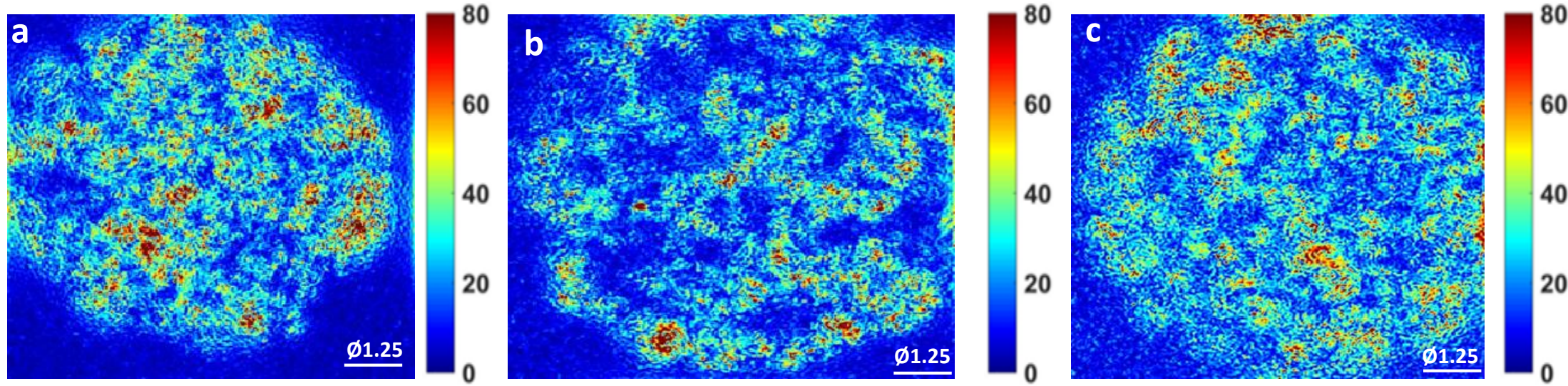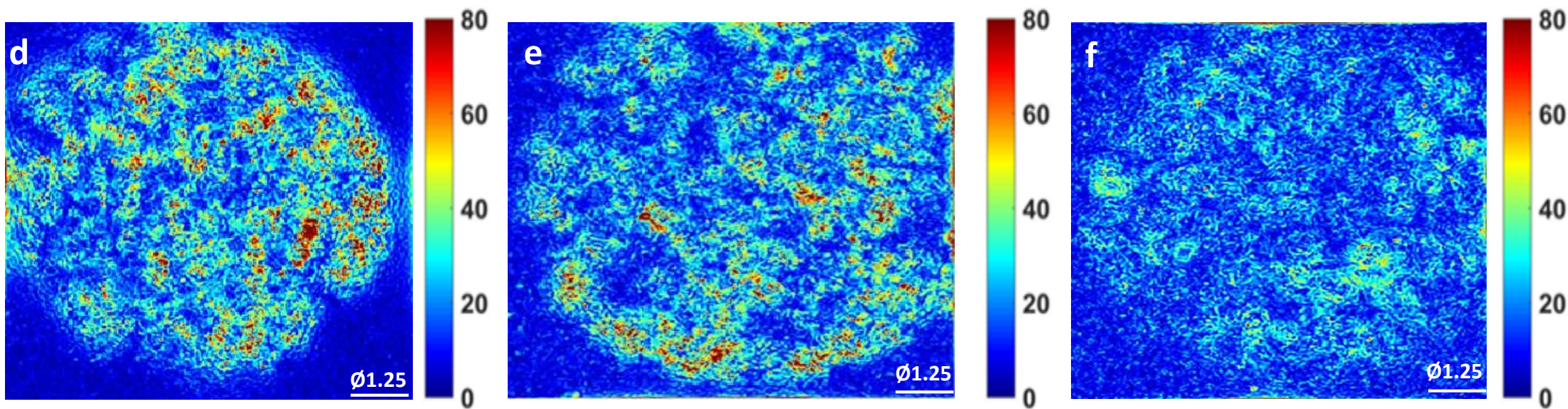
RMS tractions (Pa)

Average Normal Intercellular Stress (Pa)
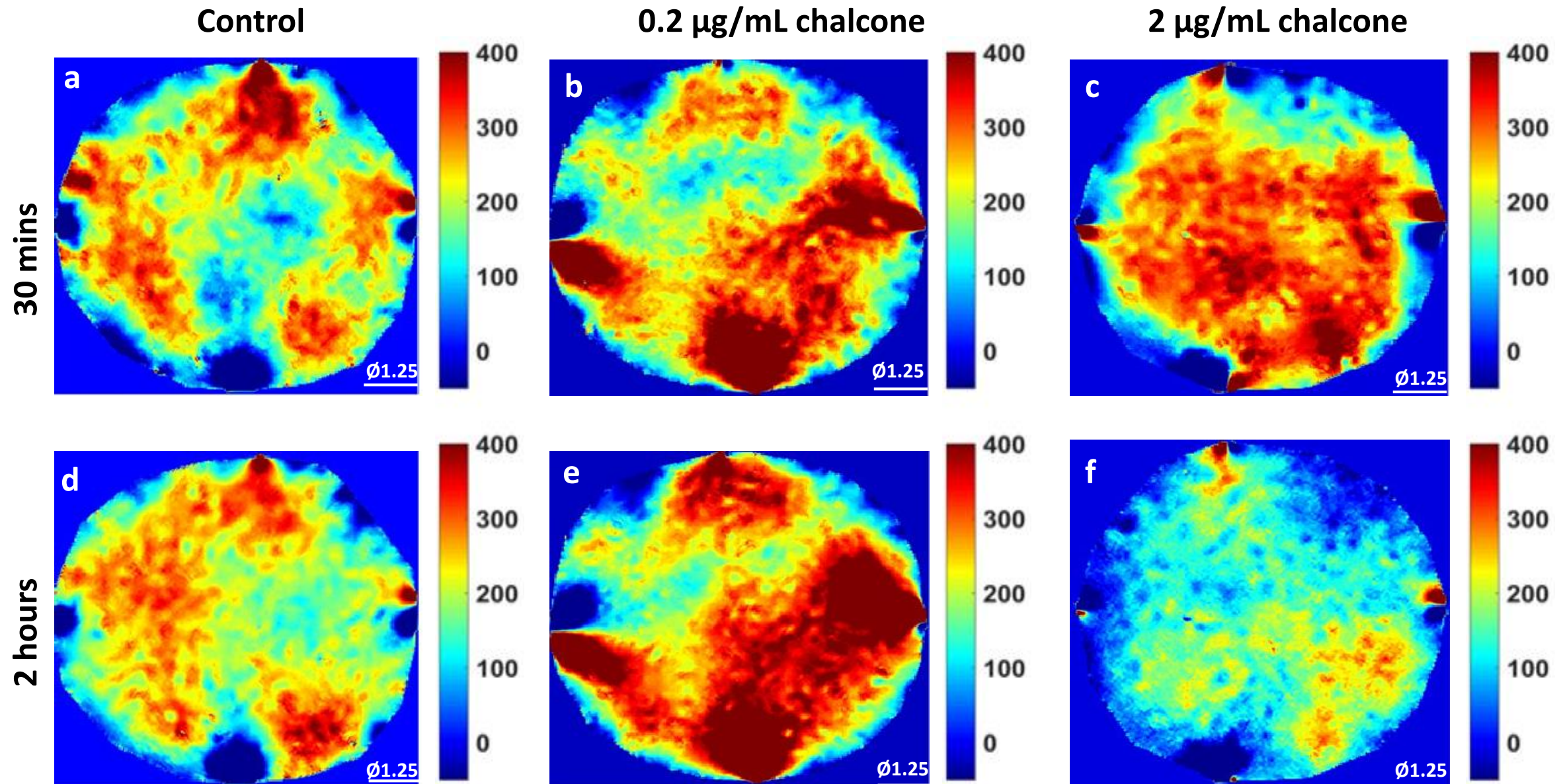
Maximum Shear Intercellular Stress (Pa)
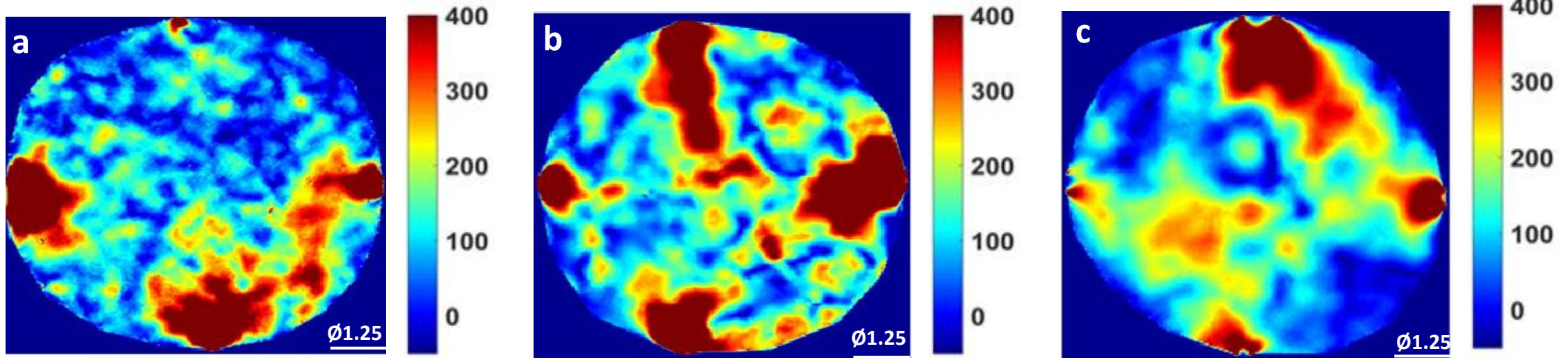
a RMS tractions (Pa) in HUVEC monolayers
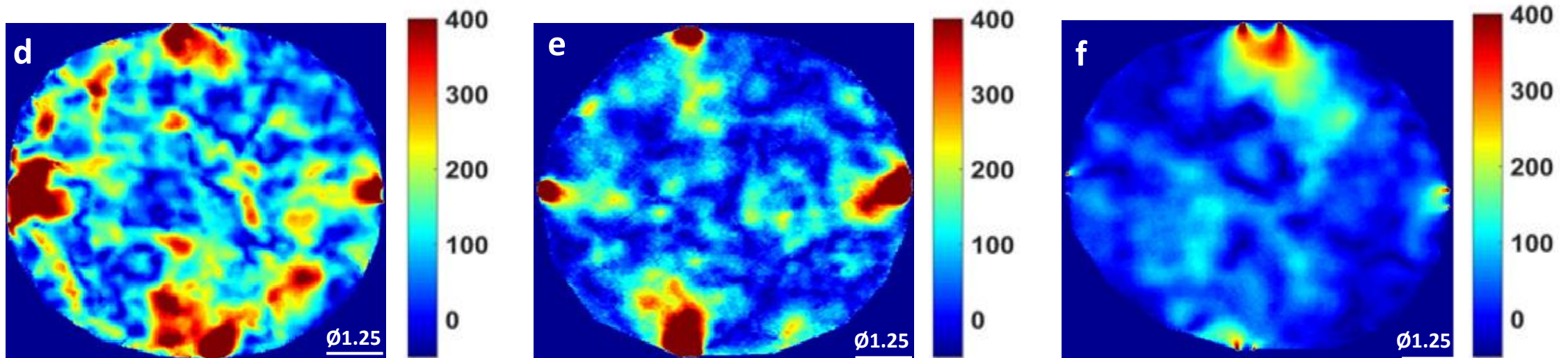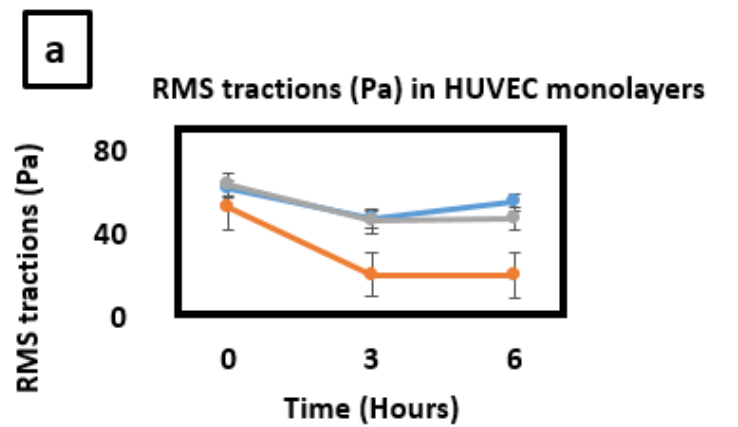
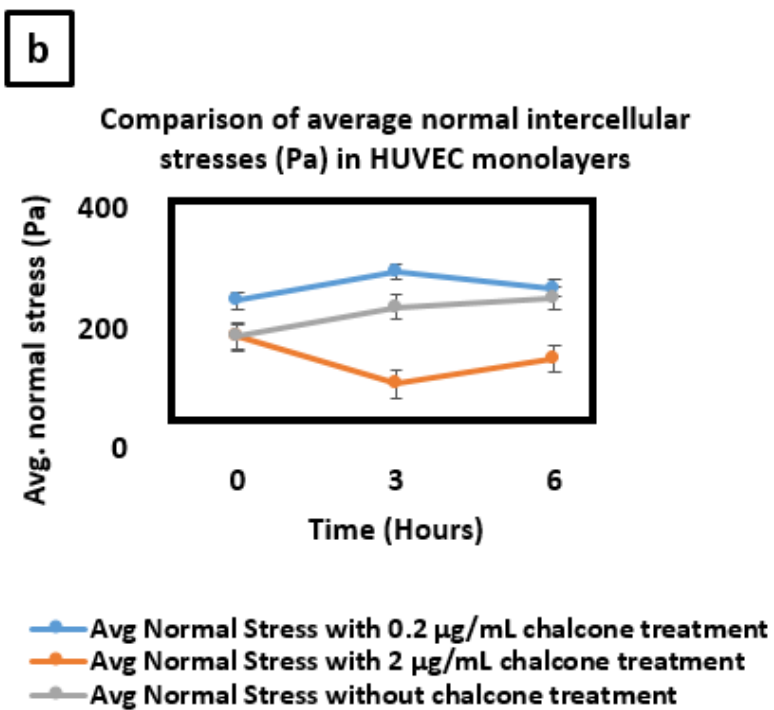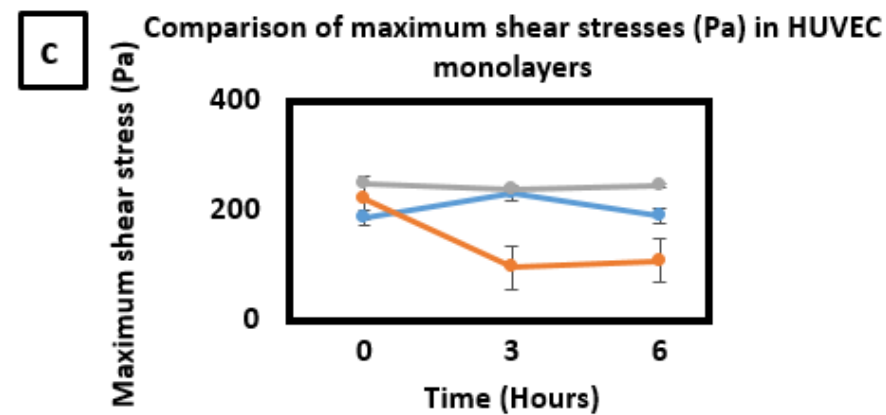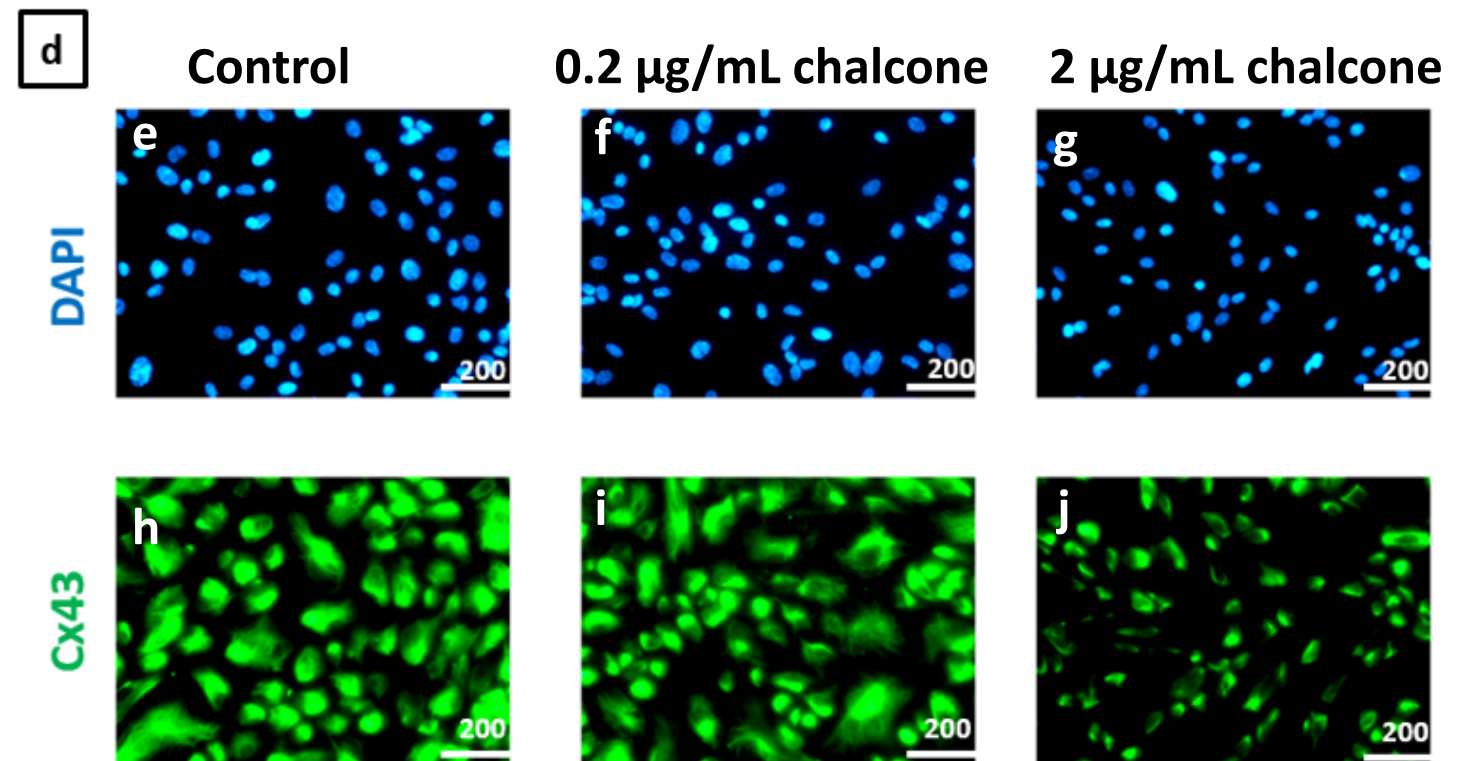—•— RMS traction with 0.2 µg/mL chalcone treatment
—•— RMS traction with 2 µg/mL chalcone treatment
—•— RMS traction without chalcone treatment

b Comparison of average normal intercellular stresses (Pa) in HUVEC monolayers

—•— Avg Normal Stress with 0.2 µg/mL chalcone treatment
—•— Avg Normal Stress with 2 µg/mL chalcone treatment
—•— Avg Normal Stress without chalcone treatment

c Comparison of maximum shear stresses (Pa) in HUVEC monolayers

—•— Maximum Shear Stress with 0.2 µg/mL chalcone treatment
—•— Maximum Shear Stress with 2 µg/mL chalcone treatment
—•— Maximum Shear Stress without chalcone treatment

d Control   0.2 µg/mL chalcone   2 µg/mL chalcone

DAPI — e / f / g

Cx43 — h / i / j

Table 1

	1200 Pa	870 Pa	1 kPa	4 kPa	6.3 kPa	11 kPa	90 kPa
Solution composition	0.05% BIS 5.5% Acryl	0.1% BIS 2% Acryl	0.03% BIS 5% Acryl	0.1% BIS 5% Acryl	0.03% BIS 10% Acryl	0.07% BIS 10% Acryl	0.3% BIS 12% Acryl
Ultra pure water	12.49 mL	13.38 mL	12.78 mL	12.255 mL	10.905 mL	10.63 mL	8.30 mL
40% Acrylamide	2.062 mL	750 µL	1.875 mL	1.875 mL	3.75 ml	3.75 mL	4.5 mL
2% BIS Acrylamide	375 µL	750 µL	225 µL	750 µL	225 µL	525 µL	2.12 mL
Fluroscent beads (0.2 µm or 0.5 µm)	80 µL	80 µL	80 µL	80 µL	80 µL	80 µL	80 µL

150 kPa
0.6% BIS
12% Acryl
5.9 mL
4.5 mL
4.5 mL
Tractions are not measurable

Table 2

		Volume	Thickness	Coverslip
20-mm sl well	Thick	500 µL	~1 mm	25 mm
	Thin	24 µL	~100 µm	18 mm
14-mm sl well	Thick	175 µL	~700 µm	18 mm
	Thin	10.3 µL	~100 µm	12 mm
14 mm 6-well	Thick	280 µL	~1.5 mm	18 mm

Name of Material/ Equipment	Company	Catalog Number	Comments/Description
18 mm coverslip	ThermoFis	18CIR-1	Essential to flatten polyacrylamide gels
2% bis-acrylamide	BIO-RAD	1610143	Component of polyacrylamide gel
2',5'-Dihydroxychalcone	SIGMA	IDF00046	To disrupt Cx43 structure
3-(Trimethoxysilyl)propyl methacrylate	SIGMA	2530-85-0	Stock solution to make bind silane mixture with
40% Acrylamide	BIO-RAD	1610140	Component of polyacrylamide gel
Acetic acid	Fisher-Sceintific	64-19-7	Essential to make bind saline solution
Alexa Fluro 488 goat anti-mouse IgG;	ThermoFisher	Catalog # A-11001	Secondary antibody
Ammonium persulfate	BIO-RAD	1610700	Polyacrylamide gel polymerizing agent
Bovine Serum Albumin (BSA)	SIGMA	9048-46-8	To make blocking solution
Bovine Type I Atelo-Collagen Solution, 3 mg/mL, 100 mL	Advance Biomatrix	5005-100ML	Use as a extracellular matrix
Corning Cell Culture Phosphate Buffered Saline (1x)	Fisher-Sceintific	21040CV	Buffer Saline needed for cell culture
Dimethyl Sulfoxide, Fisher BioReagents	Fisher-Sceintific	67-68-5	To dissolve chalcone and make stock solution
Fluoromount-G with DAPI	ThermoFisher	00-4959-52	Mounting medium for immunostaing used to st
Fluroscent microsphere Carboxylate-modified beads	ThermoFisher	F8812	0.5 micron carboxylate-modified beads (red), 2'
HEPES buffer solution 1 M	SIGMA	7365-45-9	Essential to
LVES	ThermoFisher	A1460801	Essential HUEVC media 200 supplement
Medium 200	ThermoFisher	M200500	Essential media for HUVEC cell culture
Mouse monoclonal Cx43 antibody (CX - 1B1)	ThermoFisher	Catalog # 13-8300	Primary antibody for Cx43
Petri dish (35 mm dia)	CellVis	D35-20-1.5H	35 mm petri dish with a 20 mm center well
Sulfo-SANPAH Crosslinker 100 mg	Proteochem	102568-43-4	Essential to functionalize polyacrylamide gel su

SYLGARD 184 Silicone Elastomer Kit	DOW corning	2646340	Silicon elastomer with curing agent to make PD
TEMED	BIO-RAD	1610801	Polyacrylamide gel polymerizing agent
Triton-X 100	SIGMA	9002-93-1	To permeabilize cells
Trypsin -EDTA	ThermoFisher	25300054	Used to detach cells

acetic acid and ultra-pure water

tain for DAPI

% solids

rface

MS

jove
JOURNAL OF VISUALIZED EXPERIMENTS

1 Alewife Center #200
Cambridge, MA 02140
tel. 617.945.9051
www.jove.com

ARTICLE AND VIDEO LICENSE AGREEMENT

Title of Article:	Protocol for disrupting endothelial biomechanics by Connexin 43 structural inhibition
Author(s):	M. M. Islam and R. L. Steward Jr.

Item 1: The Author elects to have the Materials be made available (as described at http://www.jove.com/publish) via:

[X] Standard Access   [ ] Open Access

Item 2: Please select one of the following items:

[X] The Author is **NOT** a United States government employee.

[ ] The Author is a United States government employee and the Materials were prepared in the course of his or her duties as a United States government employee.

[ ] The Author is a United States government employee but the Materials were NOT prepared in the course of his or her duties as a United States government employee.

ARTICLE AND VIDEO LICENSE AGREEMENT

1.   **Defined Terms.** As used in this Article and Video License Agreement, the following terms shall have the following meanings: "**Agreement**" means this Article and Video License Agreement; "**Article**" means the article specified on the last page of this Agreement, including any associated materials such as texts, figures, tables, artwork, abstracts, or summaries contained therein; "**Author**" means the author who is a signatory to this Agreement; "**Collective Work**" means a work, such as a periodical issue, anthology or encyclopedia, in which the Materials in their entirety in unmodified form, along with a number of other contributions, constituting separate and independent works in themselves, are assembled into a collective whole; "**CRC License**" means the Creative Commons Attribution-Non Commercial-No Derivs 3.0 Unported Agreement, the terms and conditions of which can be found at: http://creativecommons.org/licenses/by-nc-nd/3.0/legalcode; "**Derivative Work**" means a work based upon the Materials or upon the Materials and other pre-existing works, such as a translation, musical arrangement, dramatization, fictionalization, motion picture version, sound recording, art reproduction, abridgment, condensation, or any other form in which the Materials may be recast, transformed, or adapted; "**Institution**" means the institution, listed on the last page of this Agreement, by which the Author was employed at the time of the creation of the Materials; "**JoVE**" means MyJove Corporation, a Massachusetts corporation and the publisher of The Journal of Visualized Experiments; "**Materials**" means the Article and / or the Video; "**Parties**" means the Author and JoVE; "**Video**" means any video(s) made by the Author, alone or in conjunction with any other parties, or by JoVE or its affiliates or agents, individually or in collaboration with the Author or any other parties, incorporating all or any portion

of the Article, and in which the Author may or may not appear.

2.   **Background.** The Author, who is the author of the Article, in order to ensure the dissemination and protection of the Article, desires to have the JoVE publish the Article and create and transmit videos based on the Article. In furtherance of such goals, the Parties desire to memorialize in this Agreement the respective rights of each Party in and to the Article and the Video.

3.   **Grant of Rights in Article.** In consideration of JoVE agreeing to publish the Article, the Author hereby grants to JoVE, subject to **Sections 4** and **7** below, the exclusive, royalty-free, perpetual (for the full term of copyright in the Article, including any extensions thereto) license (a) to publish, reproduce, distribute, display and store the Article in all forms, formats and media whether now known or hereafter developed (including without limitation in print, digital and electronic form) throughout the world, (b) to translate the Article into other languages, create adaptations, summaries or extracts of the Article or other Derivative Works (including, without limitation, the Video) or Collective Works based on all or any portion of the Article and exercise all of the rights set forth in (a) above in such translations, adaptations, summaries, extracts, Derivative Works or Collective Works and (c) to license others to do any or all of the above. The foregoing rights may be exercised in all media and formats, whether now known or hereafter devised, and include the right to make such modifications as are technically necessary to exercise the rights in other media and formats. If the "Open Access" box has been checked in **Item 1** above, JoVE and the Author hereby grant to the public all such rights in the Article as provided in, but subject to all limitations and requirements set forth in, the CRC License.

612542.6   For questions, please contact us at submissions@jove.com or +1.617.945.9051.

jove
JOURNAL OF
VISUALIZED EXPERIMENTS

1 Alewife Center #200
Cambridge, MA 02140
tel. 617.945.9051
www.jove.com

ARTICLE AND VIDEO LICENSE AGREEMENT

4. **Retention of Rights in Article.** Notwithstanding the exclusive license granted to JoVE in **Section 3** above, the Author shall, with respect to the Article, retain the non-exclusive right to use all or part of the Article for the non-commercial purpose of giving lectures, presentations or teaching classes, and to post a copy of the Article on the Institution's website or the Author's personal website, in each case provided that a link to the Article on the JoVE website is provided and notice of JoVE's copyright in the Article is included. All non-copyright intellectual property rights in and to the Article, such as patent rights, shall remain with the Author.

5. **Grant of Rights in Video – Standard Access.** This **Section 5** applies if the "Standard Access" box has been checked in **Item 1** above or if no box has been checked in **Item 1** above. In consideration of JoVE agreeing to produce, display or otherwise assist with the Video, the Author hereby acknowledges and agrees that, Subject to **Section 7** below, JoVE is and shall be the sole and exclusive owner of all rights of any nature, including, without limitation, all copyrights, in and to the Video. To the extent that, by law, the Author is deemed, now or at any time in the future, to have any rights of any nature in or to the Video, the Author hereby disclaims all such rights and transfers all such rights to JoVE.

6. **Grant of Rights in Video – Open Access.** This **Section 6** applies only if the "Open Access" box has been checked in **Item 1** above. In consideration of JoVE agreeing to produce, display or otherwise assist with the Video, the Author hereby grants to JoVE, subject to **Section 7** below, the exclusive, royalty-free, perpetual (for the full term of copyright in the Article, including any extensions thereto) license (a) to publish, reproduce, distribute, display and store the Video in all forms, formats and media whether now known or hereafter developed (including without limitation in print, digital and electronic form) throughout the world, (b) to translate the Video into other languages, create adaptations, summaries or extracts of the Video or other Derivative Works or Collective Works based on all or any portion of the Video and exercise all of the rights set forth in (a) above in such translations, adaptations, summaries, extracts, Derivative Works or Collective Works and (c) to license others to do any or all of the above. The foregoing rights may be exercised in all media and formats, whether now known or hereafter devised, and include the right to make such modifications as are technically necessary to exercise the rights in other media and formats. For any Video to which this **Section 6** is applicable, JoVE and the Author hereby grant to the public all such rights in the Video as provided in, but subject to all limitations and requirements set forth in, the CRC License.

7. **Government Employees.** If the Author is a United States government employee and the Article was prepared in the course of his or her duties as a United States government employee, as indicated in **Item 2** above, and any of the licenses or grants granted by the Author hereunder exceed the scope of the 17 U.S.C. 403, then the rights granted hereunder shall be limited to the maximum rights permitted under such statute. In such case, all provisions contained herein that are not in conflict with such statute shall remain in full force and effect, and all provisions contained herein that do so conflict shall be deemed to be amended so as to provide to JoVE the maximum rights permissible within such statute.

8. **Protection of the Work.** The Author(s) authorize JoVE to take steps in the Author(s) name and on their behalf if JoVE believes some third party could be infringing or might infringe the copyright of either the Author's Article and/or Video.

9. **Likeness, Privacy, Personality.** The Author hereby grants JoVE the right to use the Author's name, voice, likeness, picture, photograph, image, biography and performance in any way, commercial or otherwise, in connection with the Materials and the sale, promotion and distribution thereof. The Author hereby waives any and all rights he or she may have, relating to his or her appearance in the Video or otherwise relating to the Materials, under all applicable privacy, likeness, personality or similar laws.

10. **Author Warranties.** The Author represents and warrants that the Article is original, that it has not been published, that the copyright interest is owned by the Author (or, if more than one author is listed at the beginning of this Agreement, by such authors collectively) and has not been assigned, licensed, or otherwise transferred to any other party. The Author represents and warrants that the author(s) listed at the top of this Agreement are the only authors of the Materials. If more than one author is listed at the top of this Agreement and if any such author has not entered into a separate Article and Video License Agreement with JoVE relating to the Materials, the Author represents and warrants that the Author has been authorized by each of the other such authors to execute this Agreement on his or her behalf and to bind him or her with respect to the terms of this Agreement as if each of them had been a party hereto as an Author. The Author warrants that the use, reproduction, distribution, public or private performance or display, and/or modification of all or any portion of the Materials does not and will not violate, infringe and/or misappropriate the patent, trademark, intellectual property or other rights of any third party. The Author represents and warrants that it has and will continue to comply with all government, institutional and other regulations, including, without limitation all institutional, laboratory, hospital, ethical, human and animal treatment, privacy, and all other rules, regulations, laws, procedures or guidelines, applicable to the Materials, and that all research involving human and animal subjects has been approved by the Author's relevant institutional review board.

11. **JoVE Discretion.** If the Author requests the assistance of JoVE in producing the Video in the Author's facility, the Author shall ensure that the presence of JoVE employees, agents or independent contractors is in accordance with the relevant regulations of the Author's institution. If more than one author is listed at the beginning of this Agreement, JoVE may, in its sole

ARTICLE AND VIDEO LICENSE AGREEMENT

discretion, elect not take any action with respect to the Article until such time as it has received complete, executed Article and Video License Agreements from each such author. JoVE reserves the right, in its absolute and sole discretion and without giving any reason therefore, to accept or decline any work submitted to JoVE. JoVE and its employees, agents and independent contractors shall have full, unfettered access to the facilities of the Author or of the Author's institution as necessary to make the Video, whether actually published or not. JoVE has sole discretion as to the method of making and publishing the Materials, including, without limitation, to all decisions regarding editing, lighting, filming, timing of publication, if any, length, quality, content and the like.

12.   **Indemnification.** The Author agrees to indemnify JoVE and/or its successors and assigns from and against any and all claims, costs, and expenses, including attorney's fees, arising out of any breach of any warranty or other representations contained herein. The Author further agrees to indemnify and hold harmless JoVE from and against any and all claims, costs, and expenses, including attorney's fees, resulting from the breach by the Author of any representation or warranty contained herein or from allegations or instances of violation of intellectual property rights, damage to the Author's or the Author's institution's facilities, fraud, libel, defamation, research, equipment, experiments, property damage, personal injury, violations of institutional, laboratory, hospital, ethical, human and animal treatment, privacy or other rules, regulations, laws, procedures or guidelines, liabilities and other losses or damages related in any way to the submission of work to JoVE, making of videos by JoVE, or publication in JoVE or elsewhere by JoVE. The Author shall be responsible for, and shall hold JoVE harmless from, damages caused by lack of sterilization, lack of cleanliness or by contamination due to
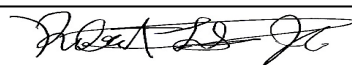
the making of a video by JoVE its employees, agents or independent contractors. All sterilization, cleanliness or decontamination procedures shall be solely the responsibility of the Author and shall be undertaken at the Author's expense. All indemnifications provided herein shall include JoVE's attorney's fees and costs related to said losses or damages. Such indemnification and holding harmless shall include such losses or damages incurred by, or in connection with, acts or omissions of JoVE, its employees, agents or independent contractors.

13.   **Fees.** To cover the cost incurred for publication, JoVE must receive payment before production and publication of the Materials. Payment is due in 21 days of invoice. Should the Materials not be published due to an editorial or production decision, these funds will be returned to the Author. Withdrawal by the Author of any submitted Materials after final peer review approval will result in a US$1,200 fee to cover pre-production expenses incurred by JoVE. If payment is not received by the completion of filming, production and publication of the Materials will be suspended until payment is received.

14.   **Transfer, Governing Law.** This Agreement may be assigned by JoVE and shall inure to the benefits of any of JoVE's successors and assignees. This Agreement shall be governed and construed by the internal laws of the Commonwealth of Massachusetts without giving effect to any conflict of law provision thereunder. This Agreement may be executed in counterparts, each of which shall be deemed an original, but all of which together shall be deemed to me one and the same agreement. A signed copy of this Agreement delivered by facsimile, e-mail or other means of electronic transmission shall be deemed to have the same legal effect as delivery of an original signed copy of this Agreement.

A signed copy of this document must be sent with all new submissions. Only one Agreement is required per submission.

CORRESPONDING AUTHOR

Name: Robert L. Steward Jr.

Department: Mechanical and Aerospace Engineering

Institution: University of Central Florida

Title: Assistant Professor

Signature: *[signature]* Date: 3/24/19

Please submit a **signed** and **dated** copy of this license by one of the following three methods:
1. Upload an electronic version on the JoVE submission site
2. Fax the document to +1.866.381.2236
3. Mail the document to JoVE / Attn: JoVE Editorial / 1 Alewife Center #200 / Cambridge, MA 02140

Response to Editor:

Protocol for perturbing endothelial biomechanics by Connexin 43 structural disruption

M. M. Islam and R. L. Steward Jr.

Editorial comments:

1. The references are not numbered in order-e.g., 31 is cited before 6. Please number references in the order they are cited in the manuscript.

Thank you for your comment. We have re-ordered the references and cited them sequentially in the manuscript.

2. The introductory paragraphs for 9.1, 9.2, and 9.3 are a bit long-please reduce in length (to 2 sentences, at most) and/or move them to the Introduction or Results, as appropriate.

Thank you for your comment. We have reduced introductory paragraph of section 9.1, 9.2 and 9.3 and moved texts into the introduction. These changes can be found in lines 57-101, highlighted in green.
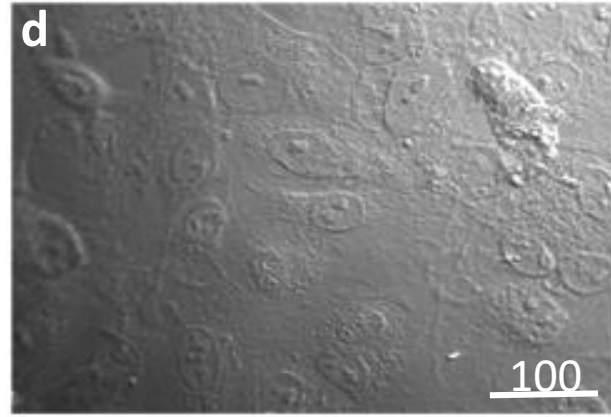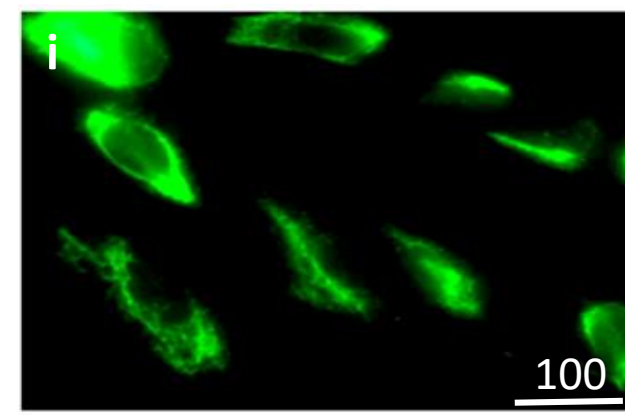
Phase contrast   **DAPI**   **Cx43**
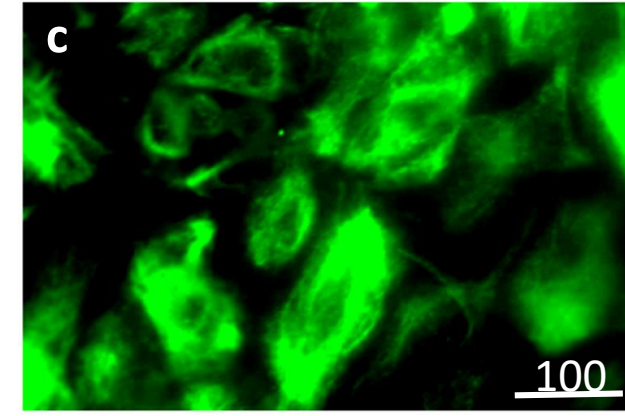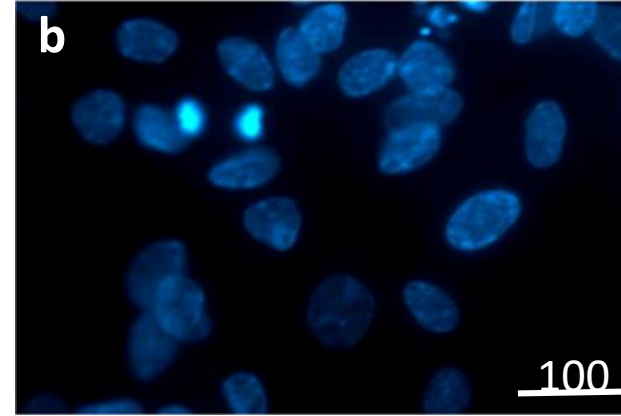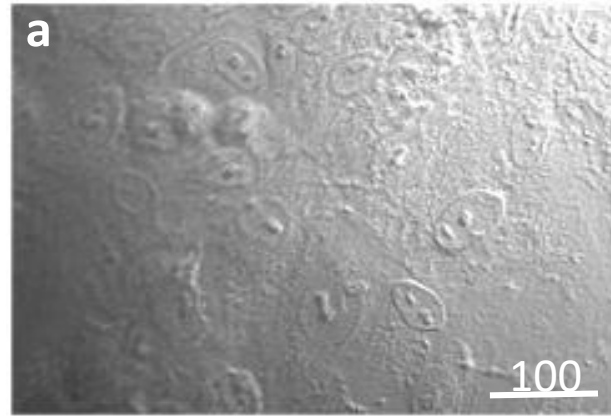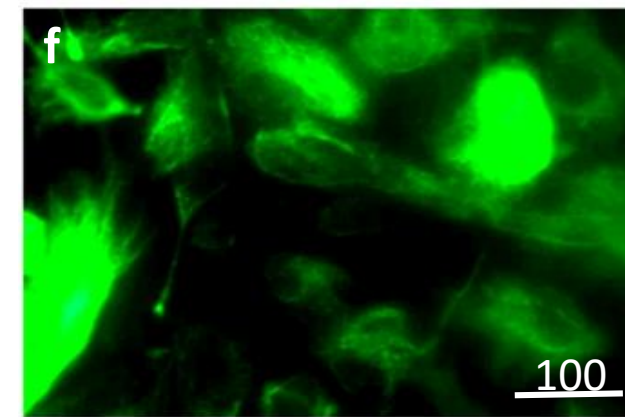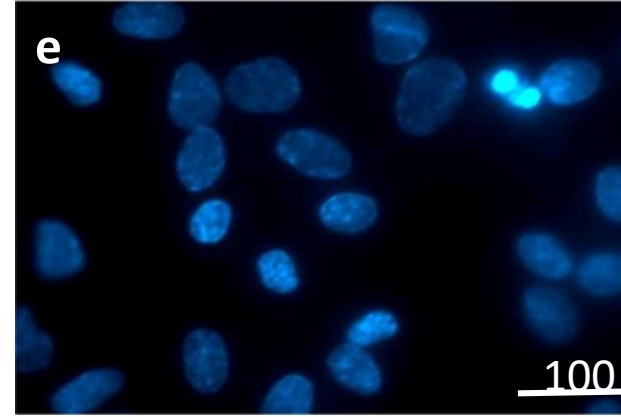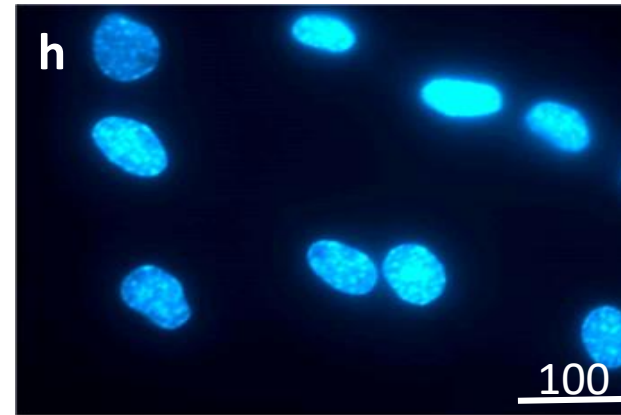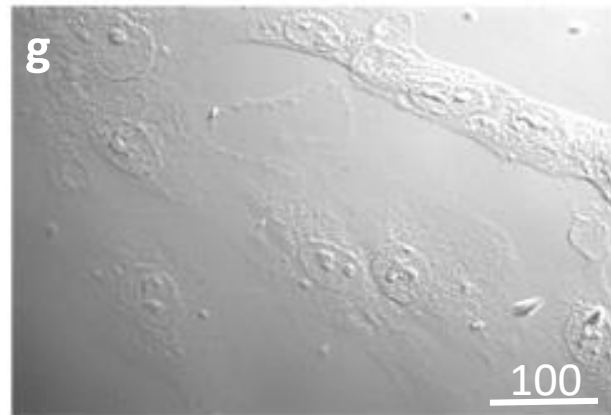
Click here to access/download
Supplemental Coding Files
supplementary materials_jove_Islam_steward.zip